European Journal of Medicinal Chemistry 85 (2014) 795–806

Contents lists available at ScienceDirect

European Journal of Medicinal Chemistry

journal homepage: http://www.elsevier.com/locate/ejmech

Original article

N-(4-[^{18}F]-fluoropyridin-2-yl)-N-{2-[4-(2-methoxyphenyl)piperazin-1-yl]ethyl}carboxamides as analogs of WAY100635. New PET tracers of serotonin 5-HT$_{1A}$ receptors

Gonzalo García [a], Valentina Abet [a], Ramón Alajarín [a], Julio Álvarez-Builla [a,*,1], Mercedes Delgado [b], Luis García-García [b], Pablo Bascuñana-Almarcha [b], Carmen Peña-Salcedo [c], James Kelly [c], Miguel A. Pozo [b,c,**,1]

[a] Departamento de Química Orgánica, Universidad de Alcalá, Alcalá de Henares, Madrid 28871, Spain
[b] CAI Cartografía Cerebral, Instituto Pluridisciplinar UCM, Paseo Juan XXIII, 1, Madrid 28040, Spain
[c] Instituto Tecnológico PET, Calle Manuel Bartolomé Cossío 10, Madrid 28040, Spain

ARTICLE INFO

Article history:
Received 28 March 2014
Received in revised form
24 July 2014
Accepted 25 July 2014
Available online 26 July 2014

Keywords:
5-HT$_{1A}$
Positron emission tomography
Fluorine-18
Radioligand
N-(4-[^{18}F]-fluoropyridin-2-yl)-N-{2-[4-(2-methoxyphenyl)piperazin-1-yl]ethyl}carboxamides

ABSTRACT

N-(4-[^{18}F]-Fluoropyridin-2-yl)-N-{2-[4-(2-methoxyphenyl)piperazin-1-yl]ethyl}-carboxamides were prepared by labeling their 4-nitropyridin-2-yl precursors through nitro substitution by the ^{18}F anion. *In vitro* and *in vivo* tests showed that the cyclohexanecarboxamide derivative is a reversible, selective and high affinity 5-HT$_{1A}$ receptor antagonist (IC_{50} = 0.29 nM, k_i = 0.18 nM) with high brain uptake, slow brain clearance and stability to defluorination when compared with conventional standards. This PET radioligand is a promising candidate for an improved *in vivo* quantification of 5-HT$_{1A}$ receptors in neuropsychiatric disorders.

1. Introduction

Molecular imaging techniques such as PET (Positron Emission Tomography) are useful tools for translational neuroscience from animal models to man. Observations carried out by this technique have suggested that there is a relationship between the serotonin 5-HT$_{1A}$ receptor and human cognition by the determination of alterations in receptor binding in patients through the imaging of receptor densities [1]. The neurotransmitter serotonin (5-hydroxytryptamine, 5-HT) and its receptors have been shown to be involved in the pathophysiology of psychiatric diseases such as schizophrenia [2], depression [3], mood disorders [4–7], and neurodegenerative processes such as Alzheimer's and Parkinson's diseases [8,9]. The 5-HT$_{1A}$ receptor has therefore been proposed as a target for the development of cognitive enhancers in the treatment of numerous cognitive dysfunction-related disorders.

An array of PET tracers has been developed for the imaging of 5-HT$_{1A}$ receptors (Fig. 1) [1,10–12]. Two antagonists have been principally studied in human diseases, namely [*carbonyl*-^{11}C]

Abbreviations: PET, positron emission tomography; 5-HT$_{1A}$, receptor 1A of 5-hydroxytryptamine; 5-HT, 5-hydroxytryptamine; WAY100635, N-{2-[4-(2-methoxyphenyl)piperazin-1-yl]ethyl}-N-(pyridin-2-yl)cyclohexanecarboxamide; MPPF, 4-fluoro-N-{2-[1-(2-methoxyphenyl)-piperazin-1-yl]ethyl}-N-(pyridin-2-yl) benzamide; k_D, apparent equilibrium dissociation constant; WAY100634, N-{2-[4-(2-methoxyphenyl)piperazin-1-yl]ethyl}pyridin-2-amine; 5-HT$_{2B}$, receptor 2BA of 5-hydroxytryptamine; $D_{4,4}$, receptor 4,4 of dopamine; SPECT, single-photon emission computed tomography; EtOH, ethyl alcohol; MW, microwaves; dba, tris(dibenzylideneacetone)dipalladium(0); BINAP, 2,2′-bis(diphenylphosphino)-1,1′-binaphthyl; IPrHCl, 1,3-bis(2,4,6-trimethylphenyl)imidazolium chloride; *t*-BuONa, sodium butoxide; CsOAc, cesium acetate; DMSO, dimethyl sulfoxide; Chx, cyclohexyl; 1-Ad, adamant-1-yl; 2-py, pyridin-2-yl; THF, tetrahydrofuran; DMF, N,N-dimethylformamide; HPLC, high-performance liquid chromatography; Ph, phenyl; IC_{50}, concentration producing 50% inhibition; k_i, inhibition constant; EOB, end-of-bombardment; 8-OH-DPAT, 2-(dipropylamino)-8-hydroxytetraline; BBB, blood–-brain barrier; BP, binding potential; ID, injected dose.

* Corresponding author.
** Corresponding author. CAI Cartografía Cerebral, Instituto Pluridisciplinar UCM, Paseo Juan XXIII, 1, Madrid 28040, Spain.
E-mail addresses: julio.alvarez@uah.es (J. Álvarez-Builla), pozo@med.ucm.es (M.A. Pozo).
[1] These authors contributed equally.

http://dx.doi.org/10.1016/j.ejmech.2014.07.096
0223-5234/

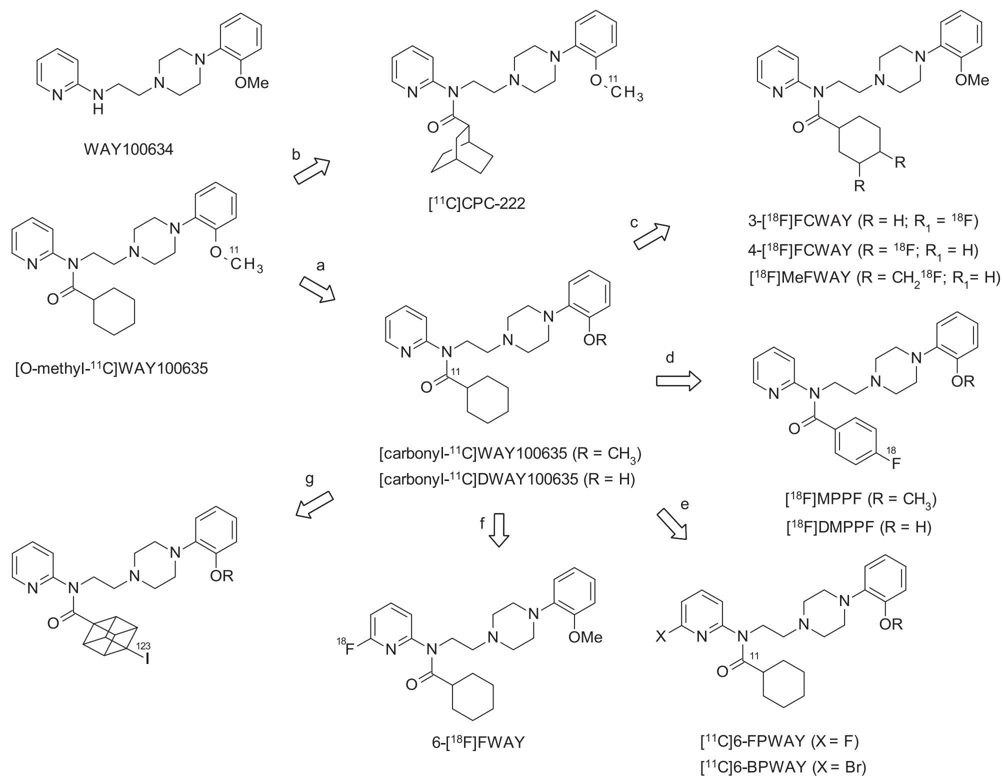

Fig. 1. Evolution of structures of PET radiotracers of 5-HT_{1A} receptors, key metabolite WAY100634 and radiolabeling methods: (a) carbonyl labeling; (b) bulky acyl group; (c) fluorine labeling on the cyclohexane ring; (d) fluorine labeling on the aromatic acyl group; (e) halogen on the pyridine C6 atom; (f) fluorine labeling on the pyridine C6 atom; (g) iodine labeling on the bulky acyl group.

WAY100635 and [^{18}F]MPPF [13,14]. WAY100635 is potent, selective and shows high affinity ($k_D = 0.2$ nM) [15]. Recent *in vitro* studies showed that WAY100635 and its major metabolite WAY100634 also have affinity for other receptors such as 5-HT_{2B} and $D_{4,4}$ [16], although this finding has not subsequently been confirmed [17]. In addition, radiolabeling with carbon-11, which has a very short half life, is a challenge to radiochemical yields, purities and specific activities [18]. [^{18}F]MPPF is a selective antagonist ($k_D = 0.34$ nM) with a longer half-life, but it shows low brain uptake compared to [*carbonyl*-^{11}C]WAY100635 (0.05% and 0.45% ID/g at 30 min in rats, respectively) and rapid metabolism *in vivo* [14,19]. In spite of its drawbacks, [*carbonyl*-^{11}C]WAY100635 remains the 'gold standard' for PET imaging of the 5-HT_{1A} receptor [20,21]. However, [^{18}F]MPPF has the advantage of being simpler to synthesize and the longer half-life of ^{18}F allows for distribution to remote facilities that do not have an in-house cyclotron. The synthesis of this compound is based on the displacement of a nitro group on a benzene ring by a weak nucleophile such as the ^{18}F anion, a process that suffers from low efficiency. However, the efficiency can be substantially improved by changing the position of the leaving group – the nitro group in this case – on the molecule.

Numerous modifications to the structures of WAY100635 and MPPF have been reported as part of the development of new PET and SPECT (Single-Photon Emission Computed Tomography) radiolabeled ligands for 5-HT_{1A} with improved specificity [22], *in vivo* kinetics [22–26] and metabolic stability [27–33] (Fig. 1). In spite of the improved parameters, the aforementioned tracers also suffer from poor radiosynthetic yields [22,23,34], low brain uptake [33], extensive *in vivo* defluorination [32,35] and hydrolysis of the amide bond [36,37]. There is therefore a need for new 5-HT_{1A} radiotracers that combine an optimal radiosynthesis process with improved pharmacological profiles and imaging properties.

We report here a series of novel analogs of WAY100634 and MPPF labeled with fluorine-18 for the quantification of 5-HT_{1A} receptors by PET imaging. These tracers all bear a [^{18}F]fluorine label on the pyridine C4 atom, which *a priori* would allow an improvement in radiolabeling efficiency, and they possess different aliphatic (cyclohexyl, adamant-1-yl), aromatic (phenyl) and heteroaromatic (pyridine-2-yl) radicals at the acyl group. The chemical synthesis of the precursors is described and we report the first radiosynthesis of these derivatives. The results of *in vitro* and *in vivo* assays of binding specificity and kinetics are also reported. One analog, the 4-[^{18}F]fluoropyridine derivative of WAY100635, was found to be a potent 5-HT antagonist and it showed good selectivity for 5-HT_{1A} receptors, higher brain uptake and slower washout than [^{18}F]MPPF, a commonly used fluorine-18 PET tracer for 5-HT_{1A}.

2. Chemistry

The synthetic route for the precursors was designed in order to build molecules with a 4-nitropyridin-2-yl moiety on which the fluorination step would subsequently be carried out (Scheme 1). Commercially available piperazine **1** was transformed into **2** and **3** in 98% yield using modifications of previously reported methods [38]. 2-Chloro-4-nitropyridine-1-oxide (**4**) was used to link amine **3** by nucleophilic substitution to give pyridine *N*-oxide **5**. Compound **5** was the only reaction product but it was obtained in low yield (31%) in spite of the harsh conditions applied (1.5 equiv of **4**, EtOH, 100 °C, 1 h, microwaves). The yield was not improved by carrying out the reaction in the presence of a stoichiometric amount of tertiary amine

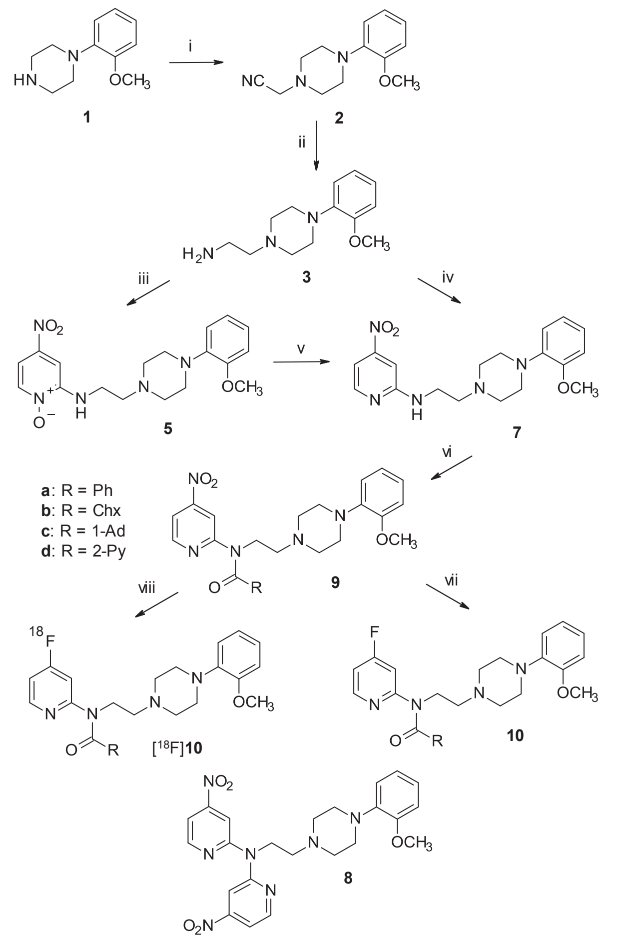

Scheme 1. Synthesis of precursors, cold derivatives and [^{18}F]-labeled derivatives. *Reagents and conditions*: (i) Bromoacetonitrile, K_2CO_3, cat NaI, acetone, reflux; (ii) $LiAlH_4$, THF, reflux; (iii) 2-chloro-4-nitropyridine-1-oxide (**4**), EtOH, MW, 100 °C; (iv) 2-chloro-4-nitropyridine (**6**), *t*-BuONa, $Pd_2(dba)_3$, BINAP, toluene, 80 °C; (v) PCl_3, CH_2Cl_2, rt; (vi) Method A (**9a**, **9b**): RCOCl, CH_2Cl_2, rt; Method B (**9c**): RCOCl, toluene, reflux; Method C (**9d**): a. RCOOH, oxalyl chloride, cat DMF, CH_2Cl_2, rt; b. **7**, toluene, 80 °C; (vii) CsF, DMSO, 180 °C; (viii) [kryptofix 2.2.2. K][^{18}F]F, DMSO, 180–200 °C.

(ethyldiisopropylamine) *vs* **3**. When the reaction was carried out under reflux, poorer results were obtained (4 h, 23%; 20 h, 17%) even though a 2-fold excess of amine **3** was used (6 h, 26%). Microwave-assisted conditions accelerated the process 6-fold (1 h MW *vs* 6 h reflux) but only a slight improvement in the yield was achieved (31% MW *vs* 26% reflux). These results were unexpected since the reaction of 2-bromo-4-nitropyridine-1-oxide was previously reported to give moderate to good yields on using methylamine (3 equiv, 73%), aniline and cyclohexylamine (2 equiv, 56% and 69%, respectively) [39,40]. Steric hindrance caused by the bulky substituent at the β-carbon to the nucleophilic amine is the most likely explanation for the low yield obtained. Pd-catalyzed C–N cross-coupling reactions were also unsuccessfully evaluated. Although this reaction has not been reported to date for *N*-oxides, we tested the reactivity of *N*-oxide **4** by conventional heating but found that the yield diminished. The reaction of **4** with **3** catalyzed by CuI or $Pd_2(dba)_3$, in the presence of BINAP or IPrHCl as ligands and *t*-BuONa or CsOAc as bases, gave lower yields of **5** when the process was carried out in DMSO (90 °C, 9%), toluene (80 °C, 21%) or 1,4-dioxane (100 °C, 14%) for 24 h [41–43]. The C–N cross-coupling reaction with 2-chloro-4-nitropyridine (**6**) using Buchwald and Nolan procedures [41,43] gave only low yields of **7** (4% and 21%, respectively) and disubstitution product **8** (8%) was also formed.

N-Oxide **5** was deoxygenated with PCl_3 to yield pyridine **7** quantitatively. Subsequent acylation of **7** gave precursors **9**. For the benzoyl (**9a**) and cyclohexanecarbonyl (**9b**) derivatives, acylation was carried out at room temperature in dichloromethane (Method A, 95% and 92% yield, respectively). For the bulky 1-adamantanecarbonyl derivative (**9c**) it was necessary to use toluene under reflux (Method B, 60%). The picolinoyl derivative (**9d**) was obtained from picolinoyl chloride, prepared *in situ* using oxalyl chloride in dichloromethane, with heating in toluene (Method C, 70%). All of the desired precursors **9a–d** were successfully prepared in low overall yields (20–30%) from commercially available **1**.

Cold fluorination experiments were performed in order to obtain standard samples of compounds **10** for the characterization of their radiolabeled counterparts and to provide samples for binding assays. Experiments were carried out by conventional and microwave-accelerated heating. The preparation of 4-fluoropyridine derivatives **10** was optimized by microwave-assisted synthesis (**9a–c**, 100 W; **9d**, 140 °C) using an excess of CsF (**9a**, **b**, **d**, 5 equiv; **9c**, 10 equiv) in DMSO (**9a–c**, 0.02 M; **9d**, 0.004 M) for 5 min (**10b**, 52%; **10c**, 70%), 3 min (**10d**, 62%) and 2 min (**10a**, 40%). The microwave-assisted procedure was up to 2-times faster and the optimal power for **10a–c** was 100 Watts, although a larger excess of fluoride was necessary for **10c** in order to achieve good conversion. For **10d**, temperature-controlled rather than power-controlled conditions were required to obtain good yields. The reaction was also optimized by classical heating (180 °C) using 5 equivalents of CsF in DMSO (**9a–d**, 0.02 M) for 10 min (**10b**, 59%),

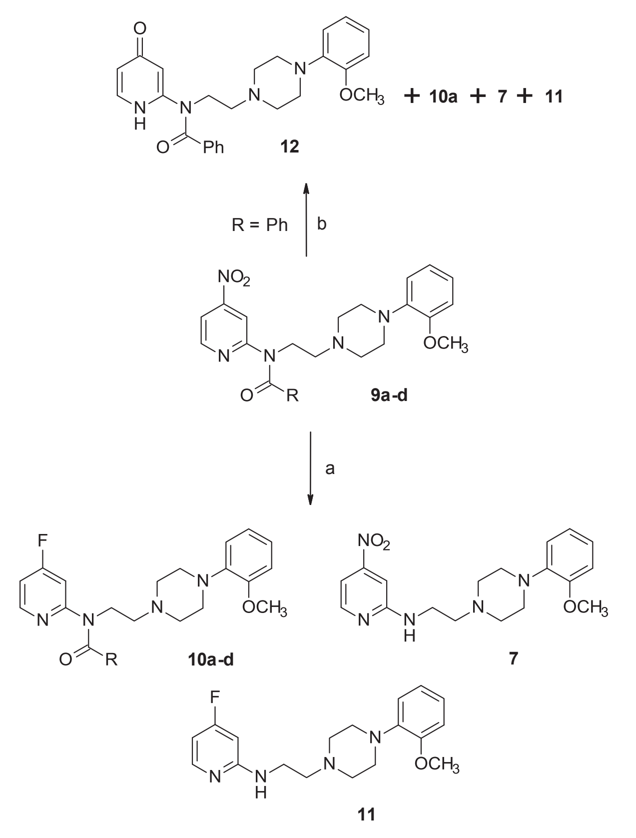

Scheme 2. Major by-products formed during cold fluorination of precursors **9a–d** and compound **12** formed in the presence of water. *Reagents and conditions*: (a) CsF (5 equiv), DMSO, 180 °C, 3–10 min; (b) CsF (5 equiv), H_2O (2.8 equiv), DMSO, 180 °C, 5 min.

5 min (**10a**, 43%; **10c**, 95%) and 3 min (**10d**, 58%). Both conventional and microwave-assisted syntheses gave deacylated starting material **7** (≤10%) and deacylated reaction product **11** (≤7%) as major by-products (Scheme 2). Since the solvent employed was rigorously dried, amide bond hydrolysis by water was ruled out. In an effort to shed light on this aspect, compound **9a** was reacted under classical conditions, as described above, in the presence of water (2.8 equiv) and a ratio of 89:4:3:4 was found for **10a**:**7**:**11**:**12** by HPLC (See Scheme 2). Compound **12** is therefore formed by the displacement of either the nitro group or fluoro-substituent by water. Fluoride ion-mediated hydrolysis is probably the origin of deacylated by-products **7** and **11**, as reported for phosphoroselenoic esters and amides [44]. In addition, the strong electron-withdrawing effect of both the 4-nitro group and the α-azine-nitrogen make the 4-nitropyridin-2-yl-amide anion a good leaving group and this potentially assists the fluorolysis. Attempts have previously been made to identify impurities formed during the radiolabeling of [^{18}F]MPPF but, as the structures of the labeled by-products could not be assigned [45], it was not possible to confirm that this fluorolysis had taken place during the radiolabeling.

3. Results and discussion

3.1. Receptor binding in vitro

3.1.1. 5-HT$_{1A}$ receptor binding

Radioligand binding experiments carried out with **10b**, which showed better imaging results both *in vitro* and *in vivo* (see below), were performed in triplicate using the 5-HT$_{1A}$ agonist [^{3}H]8-OH-DPAT [46]. Inhibition curves were measured and the concentrations that produced 50% inhibition (IC$_{50}$) were derived from non-linear regression curve fitting and apparent equilibrium inhibition constant (k_i) values were calculated according to the Cheng–Prusoff equation [47]. Compound **10b** (IC$_{50}$: 0.35 nM; k_i: 0.22 nM) is an even better 5-HT$_{1A}$ receptor antagonist than its defluorinated analog WAY-100635 (IC$_{50}$: 0.91 nM; k_i: 0.39 nM) [32,33].

3.1.2. Receptor binding profile

The selectivity of **10b** for the 5-HT$_{1A}$ receptor over a panel of seven relevant receptors was determined at a concentration of 0.55 nM and the results are shown in Table 1. Compound **10b** inhibited the 5-HT$_{1A}$ receptor between 2- to 20-fold better than other receptors tested. The lowest selectivity was found for adrenoreceptor α_{1D}.

Table 1
Inhibition of relevant receptors by **10b** at 0.55 nM ($n = 3$).

Receptor	Reference compound			Inhibition (%)
	Name	IC$_{50}$ (nM)	k_i (nM)	
5-HT$_{1A}$	[^{3}H]8-OH-DPAT	0.29	0.18	37
5-HT$_{1D}$	[^{3}H]serotonin	3.8	1.3	6
5-HT$_{2B}$	[^{3}H]mesulergine	0.49	0.27	−21[a]
5-HT$_7$	[^{3}H]serotonin	0.38	0.14	6
α_{1A}-A	[^{3}H]WB-4101	0.46	0.23	2
α_{1B}-A	[^{3}H]prazosin	0.22	0.06	4
α_{1D}-A	[^{3}H]prazosin	0.14	0.06	21
D$_4$	[^{3}H]clozapine	91	35	8

[a] Low to moderate negative values have no real meaning and are attributable to variability of the signal around the control level. High negative values (≥50%) sometimes obtained with high concentrations of test compounds are generally attributable to non-specific effects of the test compounds in the assays. On rare occasion they could suggest an allosteric effect of the test compound.

3.2. Radiolabeling

The radiolabeling of precursors **9** was accomplished by nucleophilic aromatic substitution of the nitro group by [^{18}F]fluoride in DMSO at 180–200 °C (Scheme 1) [48]. The compounds were purified by semi-preparative HPLC and the structures of labeled compounds [^{18}F]**10** were confirmed by comparison with the cold standards. Compound [^{18}F]**10a** was radiolabeled in 25.7 ± 8% yield (corrected to EOB), while compounds [^{18}F]**10b**–**d** were synthesized in 27.8 ± 8%, 25.9 ± 5% and 22.7 ± 4% yields, respectively. Specific activities were in the range 25–500 GBq/μmol. Under the same conditions [^{18}F]MPPF was radiosynthesized in 23.8 ± 9% yield.

The radiolabeling of pyridine moieties with [^{18}F]fluoride ions has previously been undertaken at the C6 carbon [49,50]. However, it has been shown that analogs of WAY100635 labeled at this position are rapidly metabolized [31]. In principle, labeling at the C4 position of the pyridine ring should be less favorable for metabolization and this hypothesis has been borne out by previously reported labeling studies [51]. It was found that fluorination at C4 is more favorable than labeling in the benzenecarboxamide moiety ([^{18}F]**10a**: 25.7% *vs* [^{18}F]MPPF: 23.8%), although the effect was small. Our radiolabeling procedure represents a significant improvement on the one reported for 6-[^{18}F]FWAY (~2% decay-corrected yield, Fig. 1) [31].

3.3. In vitro brain autoradiography

The binding patterns of [^{18}F]**10a** (not shown) and [^{18}F]**10b** (Fig. 2) were identical to those obtained with [^{18}F]MPPF and [^{3}H]8-OH-DPAT ligands and correspond to the known 5-HT$_{1A}$ receptor rat brain distribution [52]. Furthermore, in both cases the specific

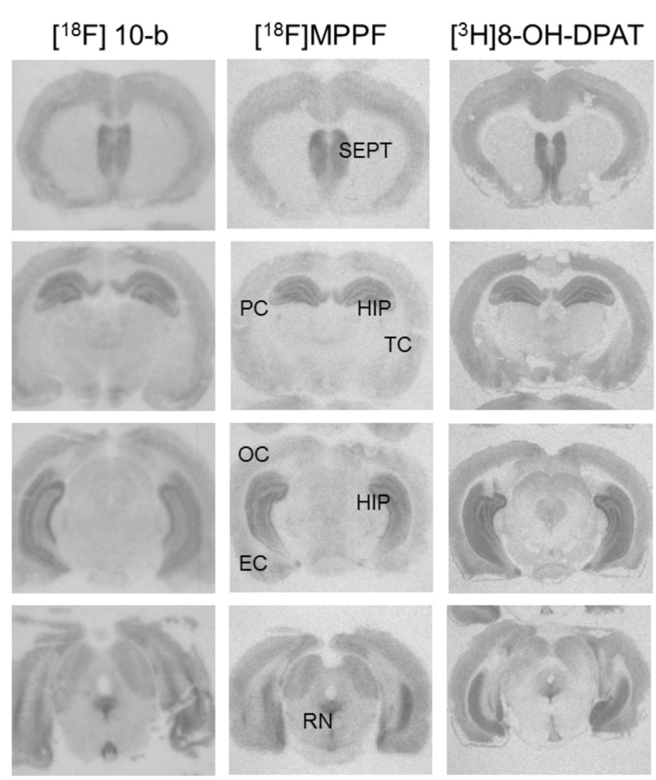

Fig. 2. *In vitro* autoradiograms of coronal brain sections of rat incubated with [^{18}F]**10b**, [^{18}F]MPPF and [^{18}F]8-OH-DPAT. SEPT, septum; PC, parietal cortex; TC, temporal cortex; HIP, hippocampus; OC, occipital cortex; EC, entorhinal cortex; RN, raphe nucleus.

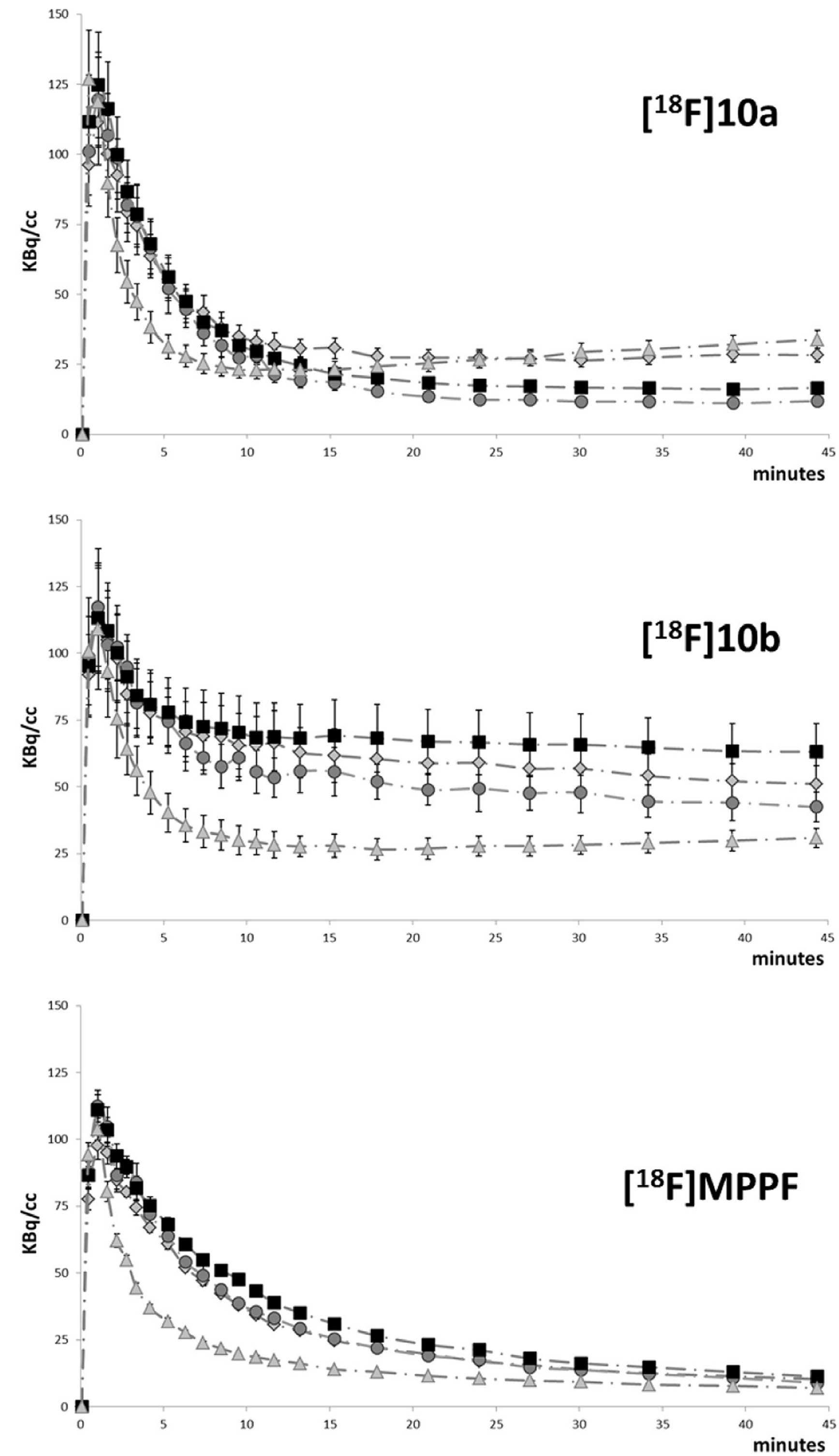

Fig. 3. Time-activity curves for [^{18}F]**10a**, [^{18}F]**10b** and [^{18}F]MPPF. PET time–activity curves in different structures measured after injecting the different tracers. Data are expressed as the mean ($n = 8$) of the average radioactivity (KBq/cc) bound in different structures (prefrontal cortex, septum, hippocampus and cerebellum) at different time points. Legend: hippocampus (squares), prefrontal cortex (diamonds), septum (circles) and cerebellum (triangles).

signal was abolished when the tracer was incubated in the presence of 1 μM WAY100635, a well characterized 5-HT$_{1A}$ antagonist. These results indicate that [^{18}F]**10a** and [^{18}F]**10b** show high selectivity for 5-HT$_{1A}$ receptors. However, compounds [^{18}F]**10c** and [^{18}F]**10d** showed high accumulation in the brain regions with poor 5-HT$_{1A}$ receptor density, such as the striatum and the thalamus. Given the reports that WAY100635 also shows some *in vitro* affinity for the 5-HT$_{2B}$ and dopamine D$_{4,4}$ receptors [16] and the similarity in structure between these derivatives and WAY100635, it is possible that non-target interactions with the dopamine system could explain the lack of specificity of these compounds for 5-HT$_{1A}$ receptors.

3.4. In vivo brain distribution studies (dynamic PET)

The brain distribution of the radiolabeled compounds was evaluated by dynamic PET. While compound [^{18}F]**10a** crossed the blood brain barrier (BBB), it showed quick washout, as a low signal was detected in the brain at 15 min post-injection. Furthermore, uptake in the cerebellum was higher than in the hippocampus and cortex at 15 min post-injection (Fig. 3). The rest of the compounds showed good brain retention, but only [^{18}F]**10b** showed a similar binding distribution to that observed in animals administered with [^{18}F]MPPF. As in the *in vitro* experiments, compounds [^{18}F]**10c** and [^{18}F]**10d** bound highly to the striatum, indicating poor selectivity for 5-HT$_{1A}$ receptors. On the basis of its favorable kinetics and selectivity for 5-HT$_{1A}$ receptors, [^{18}F]**10b** was selected for additional *in vivo* evaluation.

The dynamic PET images revealed rapid accumulation of [^{18}F]**10b** in the brain following intravenous injection. The time–activity curves showed a high uptake in 5-HT$_{1A}$ receptor-rich structures such as the hippocampus, septum and prefrontal cortex a few minutes after injection (Fig. 3). Weak binding was observed in the cerebellum, a region known to have low expression of 5-HT$_{1A}$ receptors. The average time–activity curve for [^{18}F]**10b** obtained from 8 rats is displayed in Fig. 3. Tracer uptake remains almost constant from 10 to 40 min post-injection in contrast to the [^{18}F]MPPF time–activity curve, which shows a gradual decrease over time.

One possible explanation for the rapid brain washout of [^{18}F]**10a** is that it is a substrate with high affinity for P-glycoprotein. Indeed, several 5-HT$_{1A}$ receptor radioligands with similar structures, based on an arylpiperazinyl-alkyl backbone, including [^{18}F]MPPF, are known to act as substrates for P-glycoprotein at the rat BBB [53,54]. Metabolic instability may be another contributing factor, as a low uptake of activity in the skull, consistent with *in vivo* defluorination, was observed when a 45 min dynamic PET scan was performed.

Tracers [^{18}F]**10b**, [^{18}F]**10c** and [^{18}F]**10d** did not show significant accumulation of activity in bone, although intense signal uptake in striatal tissue during the dynamic scan did reinforce the lack of specificity by [^{18}F]**10c** and [^{18}F]**10d** for 5-HT$_{1A}$ receptors observed *in vitro*. Washout of [^{18}F]**10b** from brain regions was quite slow, with the slope of the time–activity curve being small from 20 min after injection (Fig. 3), but its uptake in known 5-HT$_{1A}$ receptor-rich regions was similar to that of [^{18}F]MPPF. The uptake ratios of [^{18}F]**10b** and [^{18}F]MPPF in several brain regions *vs* the cerebellum at 45 min is shown in Table 2.

Uptake ratios for [^{18}F]**10b** and [^{18}F]MPPF are similar in the hippocampus, but [^{18}F]**10b** shows a higher ratio in the cortex. The hippocampus-to-cerebellum ratio reaches a maximum between 10 and 12 min for [^{18}F]MPPF (reaching a value of 2.44 ± 0.07), at which time the corresponding ratio for [^{18}F]**10b** is 2.34 ± 0.09. While the ratio for [^{18}F]MPPF begins to diminish after 12 min, the ratio for [^{18}F]**10b** slowly increases before reaching a maximum value of 2.53 ± 0.13 at 18 min. This ratio exceeds the values reported for new 5-HT$_{1A}$ tracers [54].

The binding potential (BP) parametric maps for [^{18}F]**10b** obtained by using the simplified reference tissue model (Fig. 4) enabled the BP values in several regions of interest to be calculated.

Table 2
Uptake ratios at 45 min for [^{18}F]**10b** and [^{18}F]MPPF in selected brain regions *vs* cerebellum.

Brain region	[^{18}F]**10b** ($n = 8$)	[^{18}F]MPPF ($n = 8$)
Hippocampus	1.67 ± 0.13	1.48 ± 0.06
Septum	1.15 ± 0.24	1.28 ± 0.03
Cortex	2.04 ± 0.15(*)	1.60 ± 0.05

Data are presented as a ratio ± SD of uptake (kBq/cc) in 5-HT$_{1A}$ receptor-rich brain regions *vs* cerebellum at 45 min after injection. (*) $P < 0.05$ (non-paired *t*-test).

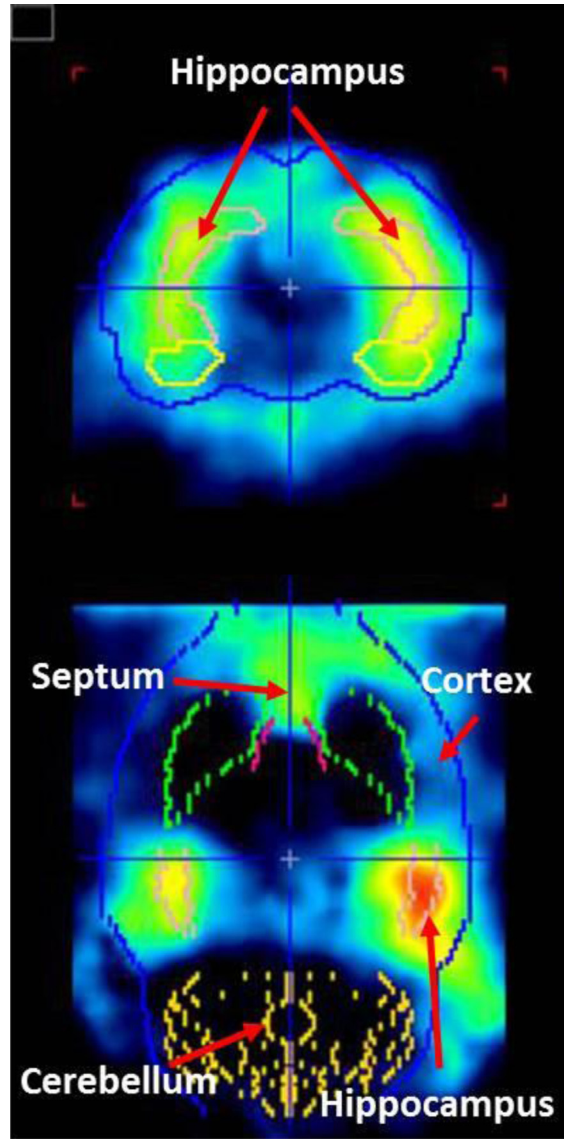

Fig. 4. Representative BP parametric map for [^{18}F]**10b**. Coronal view (top panel) and transversal view (bottom panel).

The BP values for [^{18}F]**10b** are significantly higher than those found for [^{18}F]MPPF (Table 3), with the hippocampus showing the highest BP value (1.412 ± 0.077 *vs* 0.872 ± 0.035).

The BP values of [^{18}F]**10b** taken from the parametric maps obtained in 5-HT$_{1A}$-rich brain regions are significantly higher than those found for [^{18}F]MPPF (Table 3). The highest values were observed in the hippocampus and the prefrontal cortex and these were 1.62 and 1.71 times higher ($P < 0.01$), respectively, than the values reported for [^{18}F]MPPF. The binding potential of [^{18}F]**10b** in the cerebellum was elevated with respect to that of [^{18}F]MPPF, possibly reflecting the fact that [^{18}F]**10b** binds the few 5-HT$_{1A}$ receptors in this region with higher affinity. Collectively these results demonstrate that the affinity of [^{18}F]**10b** is higher than that of [^{18}F]MPPF for the 5-HT$_{1A}$ receptor.

3.5. In vivo competition studies

The specificity of [^{18}F]**10b** for 5-HT$_{1A}$ receptors was assessed by carrying out dynamic PET studies with [^{18}F]**10b** in adult rats in the presence of 8-OH-DPAT, WAY100635, or with cold **10b** as

Table 3
[^{18}F]**10b** BP values in several brain regions of interest *vs* [^{18}F]MPPF.

Brain region	[^{18}F]**10b** BP ($n = 10$)	[^{18}F]MPPF BP ($n = 8$)
Prefrontal cortex	1.039 ± 0.082	0.608 ± 0.036
Septum	0.675 ± 0.026	0.677 ± 0.039
Caudate putamen	0.470 ± 0.028	0.386 ± 0.025
Amygdala	0.784 ± 0.051	0.477 ± 0.023
Hippocampus	1.412 ± 0.077	0.872 ± 0.035
Thalamus	0.373 ± 0.029	0.404 ± 0.027
Cerebellum	0.234 ± 0.017	0.084 ± 0.004
Brain stem	0.225 ± 0.046	0.118 ± 0.013
Whole brain	0.664 ± 0.035	0.362 ± 0.016

displacers. Cold **10b** was found to induce a dose-dependent decrease in the [^{18}F]MPPF binding potential. The BP values for [^{18}F]**10b** when simultaneously administered with one of the three aforementioned cold ligands are shown in Table 4. The binding of [^{18}F]**10b** was almost completely reversed when it was co-administered with WAY100635 or cold **10b**. The BP of [^{18}F]**10b** in the hippocampus and prefrontal cortex in these displacement experiments was reduced by 96.25% and 95.38% ($P < 0.01$), respectively, after administration of the cold ligand **10b** (0.5 mg/kg). The co-administration of the selective antagonist WAY100635 (1 mg/kg) with [^{18}F]**10b** decreased hippocampal and cortex binding by 99.15% and 95.77% ($P < 0.01$), and the hippocampus/cerebellum and prefrontal cortex/cerebellum ratios from 6.03 to 0.04 and 4.44 to 0.15, respectively. These results are consistent with the reversible binding of [^{18}F]**10b** to 5-HT$_{1A}$ receptors.

In the case of co-administration with 8-OH-DPAT at a dose of 1 mg/kg, the decreases were 61.05% and 61.02% ($P < 0.01$) in the hippocampus and frontal cortex, respectively. The smaller decreases observed in these cases are probably due to the lower affinity of 8-OH-DPAT for 5-HT$_{1A}$ receptors in comparison to WAY100635, as demonstrated in pharmacological studies [55,56].

3.6. *Biodistribution in rats*

The uptake and washout kinetics of [^{18}F]**10b** in rat were evaluated by carrying out a biodistribution experiment in normal male rats. Compound [^{18}F]**10b** displayed a high initial brain uptake (0.90% ID/g) at just 1 min post-injection. The radioactivity in the brain displayed a moderate washout rate (0.34% ID/g at 30 min) with a brain 1 min/brain 30 min ratio of 1.7.

It can be seen from the results in Table 5 that [^{18}F]**10b** was simultaneously taken up in several other organs. The distribution of the radiotracer in the liver and kidneys was initially high (1.34 and 0.81% ID/g at 15 min, respectively) and the tracer was subsequently washed out at a moderate rate (0.72 and 0.46% ID/g at 30 min). However, radioactivity was observed to accumulate within the small intestine over time (the uptake increased from 7.6% ID/g at 15 min to 13.2% ID/g at 30 min), while elevated concentrations were also observed in the kidneys and liver. These distributions probably reflect the involvement of these organs in the metabolism and excretion of the compound. Total activity in the small intestine continued to accumulate up to 30 min after injection, but in other tissues the concentration peaked at 15 min post-injection. The relatively constant activity in the brain up to 60 min provides further evidence of the slow washout of the radiolabeled compound.

Table 4
BP values for [^{18}F]**10b** when simultaneously administered with three cold ligands.

Brain region	[^{18}F]**10b**		
	8-OH-DPAT (1 mg/kg)	**10b** (0.5 mg/kg)	WAY100635 (1 mg/kg)
Prefrontal cortex	0.405 ± 0.089	0.048	0.044
Septum	0.183 ± 0.061	0.001	0.014
Caudate putamen	0.195 ± 0.043	0.018	0.022
Amygdala	0.359 ± 0.071	0.106	0.063
Hippocampus	0.550 ± 0.103	0.053	0.012
Thalamus	0.123 ± 0.029	0.021	0.010
Cerebellum	0.184 ± 0.036	0.244	0.286
Brain stem	0.207 ± 0.079	0.086	0.080
Whole brain	0.354 ± 0.053	0.186	0.261

Table 5
Average tissue distribution *vs* time (in %ID) of [^{18}F]**10b**.

Tissue	Time (min)			
	15	30	60a	120
Kidneys	0.814 ± 0.187	0.463 ± 0.068	0.285 ± 0.074	0.133 ± 0.012
Heart	0.325 ± 0.038	0.153 ± 0.013	0.076 ± 0.012	0.032 ± 0.001
Spleen	0.303 ± 0.032	0.168 ± 0.003	0.103 ± 0.013	0.049 ± 0.007
Lungs	0.344 ± 0.057	0.212 ± 0.005	0.118 ± 0.001	0.044 ± 0.008
Muscle (soleus)	0.160 ± 0.005	0.094 ± 0.002	0.061 ± 0.10	0.031 ± 0.000
Retroper. fat	0.327 ± 0.043	0.335 ± 0.042	0.321 ± 0.037	0.271 ± 0.005
Small intestine	7.559 ± 3.478	13.188 ± 0.085	1.443 ± 0.374	0.680 ± 0.201
Liver	1.337 ± 0.176	0.716 ± 0.208	0.589 ± 0.002	0.326 ± 0.025
Stomach	0.567 ± 0.041	0.247 ± 0.081	0.239 ± 0.018	0.174 ± 0.072
Whole brain	0.412 ± 0.051	0.380 ± 0.023	0.303 ± 0.022	0.075 ± 0.021
Large intestine	0.243 ± 0.027	0.160 ± 0.004	0.214 ± 0.012	0.845 ± 0.605

4. Conclusions

Four new 4-[^{18}F]fluoropyridine-labeled derivatives of WAY100635 bearing benzoyl ([^{18}F]**10b**), cyclohexanecarbonyl ([^{18}F]**10b**), adamantane-1-carbonyl ([^{18}F]**10c**) and pyridine-2-carbonyl ([^{18}F]**10d**) groups were radiosynthesized by nucleophilic displacement of the nitro group of 4-nitropyridine precursors. Yields in the range 22.7%–27.8% (corrected to EOB) were obtained and [^{18}F]**10b** was obtained in the highest yield after a synthesis time of 105 min. The nitro precursors were prepared in modest yields (20–30%) by a new approach involving a pyridine-*N*-oxide intermediate. Cold fluorination experiments showed that amide fluorolysis is the main pathway to impurities.

Labeled compounds [^{18}F]**10a–d** were evaluated as 5-HT$_{1A}$ radioligands *in vitro* and *in vivo*. Compounds [^{18}F]**10a** and [^{18}F]**10b** showed good *in vitro* distribution to 5-HT$_{1A}$-rich regions while [^{18}F]**10c** and [^{18}F]**10d**, in contrast, showed poor selectivity for the 5-HT$_{1A}$ receptor, with considerable uptake observed in 5-HT$_{1A}$-poor regions such as the striatum and the cerebellum. [^{18}F]**10a** was found to undergo rapid brain clearance and evidence for the loss of fluorine was found *in vivo*. [^{18}F]**10b** was shown to reversibly and selectively bind 5-HT$_{1A}$ receptors with high affinity. This compound has a low rate of brain clearance and evidence for radiodefluorination was not found. Compound **10b** was found to be a potent and selective 5-HT$_{1A}$ receptor antagonist by *in vitro* binding experiments.

On the basis of its high affinity and good selectivity for 5-HT$_{1A}$ receptors, [^{18}F]**10b** was identified as a promising candidate for PET imaging of the serotonergic pathway. It is envisioned that its slow brain washout makes [^{18}F]**10b** suitable for the static study and quantification of 5-HT$_{1A}$ receptor densities as part of the *in vivo* study of neuropsychiatric disorders.

5. Experimental section

5.1. *Chemistry*

Solvents (HPLC quality, Scharlau) were dried in a Solvent Purification System (MBraun) by passage through a pre-activated alumina column or were purchased with anhydrous quality. Reagents were purchased from Sigma–Aldrich and they were used as received.

Reactions involving moisture-sensitive compounds were performed under an atmosphere of dry argon. Microwave-assisted reactions were carried out in a 5 mL vial using an Initiator 2.5 synthesizer (Biotage). The reactions were monitored by thin-layer chromatography (TLC) on silica-coated aluminum sheets (Alugram silica gel 60 F_{254}). The compounds were visualized by UV light (254 nm). Purification by column chromatography was undertaken with Merck silica gel (0.030–0.075 mm) and the solvents were used as received (Scharlau). Infrared spectra (IR, NaCl windows) were recorded on a Perkin–Elmer FTIR 1725X instrument. The frequencies (ν) of the more intense bands are given in cm^{-1}. Nuclear magnetic resonance spectra (^1H and ^{13}C NMR) were recorded using Varian Gemini 200 (200 and 50 MHz, respectively), Varian Mercury-VX-300 MHz (300 and 75 MHZ, respectively) and Varian-UNITY^{PLUS}-500 (500 and 125 MHz, respectively) instruments. Chemical shifts (δ) are given in ppm and are referenced to the residual signal of the non-deuterated solvent. Coupling constants (J) are given in Hz. Elemental analyses (C, H, N) were carried out on a LECO CHNSO-932 elemental analyzer and the results were within ±0.4% of the theoretical values. All compounds were analyzed by tandem HPLC-MS. HPLC was performed on a C18, 3 μm column (Luna, Phenomenex, 3 × 100 mm) using a gradient of MeOH/water-4% formic acid at a flow rate of 1.0 mL/min. Products were detected at λ = 254 nm. Mass spectra were recorded on a Hewlett–Packard 5988A mass spectrometer. High-resolution mass spectra were recorded on an Agilent 6210 LC/MS TOF mass spectrometer.

The Supplementary data section includes experimental procedures and characterization data for compounds **2**, **3**, **5**, **7** and **8**, radiochromatograms for crude radiotracers [^{18}F]**10a–d** and additional *in vivo* brain distribution data (dynamic PET): PET/CT images of [^{18}F]**10a–d** and [^{18}F]MPPF; Time-activity curves for [^{18}F]**10c** and [^{18}F]**10d**. The synthesis of precursors **9a–d**, **10a–d** and the radiosynthesis of [^{18}F]**10a–d** are described below.

5.2. General procedures for the synthesis of *9a–d*

Method A: In a 25 mL round-bottomed flask a solution of pyridylamine **7** (500 mg, 1.40 mmol) and Et_3N (0.24 mL, 1.68 mmol) in anhydrous dichloromethane (15 mL) was prepared. The corresponding acyl chloride (1.54 mmol) was added. The mixture was stirred for 24 h at room temperature and the solvent was evaporated. The residue was purified by silica gel flash chromatography using ethyl acetate/hexane (1:1) as eluent. Amides **9** were obtained as yellowish oils.

Method B: In a 25 mL round-bottomed flask a solution of pyridylamine **7** (357 mg, 1.00 mmol) and NEt_3 (0.21 mL, 1.50 mmol) was prepared in anhydrous toluene (15 mL). The acyl chloride (1.50 mmol) was added. The mixture was stirred for 24 h at 110 °C and the solvent was evaporated. The residue was purified by silica gel column flash chromatography using ethyl acetate as eluent. Amides **9** were obtained as yellowish oils.

Method C: Oxalyl chloride (0.11 mL, 1.3 mmol) and a catalytic amount of dry DMF were added to a solution of the acid (1.2 mmol) in dry dichloromethane (5 mL) at 0 °C. The reaction mixture was stirred for 2 h at room temperature. This solution was added dropwise to a solution of the amine **7** (357 mg, 1 mmol) and NEt_3 (0.18 mL, 1.3 mmol) in dry toluene (10 mL). The mixture was heated for 24 h at 80 °C and then purified by silica gel flash chromatography using ethyl acetate as eluent. Amides **9** were obtained as yellowish oils.

5.2.1. N-{2-[4-(2-methoxyphenyl)piperazin-1-yl]ethyl}-N-(4-nitropyridin-2-yl)benzamide (*9a*)

Yield: 614 mg, 95% (method A); ^1H NMR (200 MHz, $CDCl_3$): δ 8.65 (1H, d, J = 5.5 Hz, $H6_{py}$), 7.72 (2H, m, $H5_{py} + H_{Ar}$), 7.50–7.26 (5H, m, H_{Ar}), 7.06–6.92 (4H, m, H_{Ar}), 4.39 (2H, t, J = 6.2 Hz, CH_2NCO), 3.87 (3H, s, OCH_3), 2.93 (4H, br. s, 2× CH_2N), 2.83 (2H, t, J = 6.2 Hz, CH_2N), 2.67 (4H, m, 2× CH_2N) ppm. ^{13}C NMR (50 MHz, $CDCl_3$): δ 170.9, 158.5, 153.8, 151.9, 149.8, 140.9, 135.1, 130.6, 128.2 (×2), 122.7, 120.7, 117.8, 114.3, 112.2, 110.9, 56.6, 55.1, 53.1, 50.4, 45.5 ppm. Anal. ($C_{25}H_{28}N_5O_4$) theoretical: C, 69.42; H, 6.10; N, 15.14. Found: C, 69.74; H, 6.21; N, 14.83. IR (ν_{max}, NaCl): 2941, 2818, 1661, 1574, 1534, 1500, 1465, 1355, 1304, 1240, 1141, 1022, 911, 733 cm^{-1}. HRMS (ESI-TOF): Calculated for $C_{25}H_{28}N_5O_4$ $[M+H]^+$: 462.2141. Found: 462.2145.

5.2.2. N-{2-[4-(2-methoxyphenyl)piperazin-1-yl]ethyl}-N-(4-nitropyridin-2-yl)-cyclohexanecarboxamide (*9b*)

Yield: 601 mg, 92% (method A). ^1H NMR (200 MHz, $CDCl_3$): δ 8.68 (1H, d, J = 5.5 Hz, $H6_{py}$), 8.31 (1H, dd, J = 1.7 Hz, J = 5.5 Hz, $H5_{py}$), 7.82 (1H, d, J = 1.7 Hz, $H3_{py}$), 7.02–6.80 (4H, m, H_{Ar}), 4.07 (2H, t, J = 6.4 Hz, CH_2NCO), 3.82 (3H, s, OCH_3), 2.97 (4H, br. s, 2× CH_2N), 2.65 (6H, m, 3× CH_2N), 2.44 (1H, br. dt, H_{chx}), 1.90–1.00 (10H, m, H_{chx}) ppm. ^{13}C NMR (50 MHz, $CDCl_3$): δ 176.4, 154.3, 151.7, 149.7, 140.5, 122.5, 120.5, 117.7, 113.8, 112.9, 110.6, 65.5, 54.9, 53.0, 50.0, 44.7, 42.4, 30.5, 29.2, 25.1 ppm. Anal. ($C_{25}H_{34}N_5O_4$) theoretical: C, 64.08; H, 7.31; N, 14.95. Found: C, 64.23; H, 7.40; N, 14.77. IR (ν_{max}, NaCl): 2932, 2853, 1670, 1536, 1500, 1451, 1388, 1355, 1241, 1146, 1027, 737. HRMS (ESI-TOF): Calculated for $C_{25}H_{34}N_5O_4$ $[M+H]^+$: 468.2611. Found: 468.2612.

5.2.3. N-{2-[4-(2-methoxyphenyl)piperazin-1-yl]ethyl}-N-(4-nitropyridin-2-yl)adamantane-1-carboxamide (*9c*)

Yield: 467 mg, 60% (method B). ^1H NMR (500 MHz, $CDCl_3$): δ 8.66 (1H, d, J = 5.4 Hz, $H6_{py}$), 8.11 (1H, d, J = 1.9 Hz, $H3_{py}$), 7.86 (1H, dd, J = 1.9 Hz, J = 5.4 Hz, $H5_{py}$), 6.96 (1H, m, H_{Ar}), 6.88 (2H, t, J = 4.1 Hz, $H4_{Ar}$ and $H5_{Ar}$), 6.82 (1H, d, J = 7.9 Hz, $H6_{Ar}$), 3.92 (2H, t, J = 7.9 Hz, CH_2NCO), 3.82 (3H, s, OCH_3), 2.98 (4H, m, 2× CH_2N), 2.62 (6H, m, 3× CH_2N), 1.88 (4H, m, H_{Ad}), 1.76 (2H, d, J = 2.8 Hz, H_{Ad}), 1.60 (3H, d, J = 11.7 Hz, H_{Ad}), 1.52 (3H, d, J = 11.7 Hz, H_{Ad}) ppm. ^{13}C NMR (125 MHz, $CDCl_3$): δ 180.6, 159.9, 155.1, 152.2, 150.2, 141.1, 122.9, 121.0, 118.1, 114.8, 114.0, 111.1, 56.6, 55.3, 53.5, 50.4, 48.6, 44.6, 40.1, 36.3, 28.2 ppm. Anal. ($C_{29}H_{38}N_5O_4$) theoretical: C, 66.9; H, 7.36; N, 13.45. Found: C, 67.23; H, 7.27; N, 13.5. IR (ν_{max}, NaCl): 1674, 1534, 1500, 1411, 1355, 1240, 1147, 1023, 737 cm^{-1}. HRMS (ESI-TOF): Calculated for $C_{29}H_{38}N_5O_4$ $[M+H]^+$: 520.2924. Found: 520.2930.

5.2.4. N-{2-[4-(2-hydroxyphenyl)piperazin-1-yl]ethyl}-N-(3-nitrophenyl)pyridine-2-carboxamide (*9d*)

Yield: 323 mg, 70% (method C). ^1H NMR (300 MHz, $CDCl_3$): δ 8.50 (1H, d, J = 5.3 Hz, $H6_{py}$), 8.22 (1H, d, J = 3.9 Hz, $H3_{py}$), 7.88 (2H, m, $H5_{py} + H6_{py}$), 7.77 (1H, td, J = 1.9 Hz, J = 7.9 Hz, $H4_{py}$), 7.69 (1H, dd, J = 1.9 Hz, J = 5.6 Hz, $H3_{py}$), 7.23 (1H, m, $H5_{py}$), 6.95–6.84 (4H, m, H_{Ar}), 4.32 (2H, t, J = 6.2 Hz, CH_2NCO), 3.81 (3H, s, OCH_3), 2.87 (4H, m, 2× CH_2N), 2.79 (2H, t, J = 6.3 Hz, CH_2N), 2.61 (4H, m, 2× CH_2N) ppm. ^{13}C NMR (75 MHz, $CDCl_3$): δ 168.9, 159.0, 154.4, 152.8, 152.1, 149.7, 147.8, 141.0, 137.1, 125.1, 124.9, 122.9, 120.9, 118.0, 113.7, 112.6, 111.0, 56.7, 55.2, 53.3, 50.5, 46.1 ppm. Anal. ($C_{24}H_{27}N_6O_4$) theoretical: C, 62.19; H, 5.87; N, 18.13. Found: C, 62.24; H, 6.12; N, 17.77. IR (ν_{max}, NaCl): 2818, 1661, 1574, 1532, 1500, 1463, 1354, 1240, 1143, 1024, 912, 745 cm^{-1}. HRMS (ESI-TOF): Calculated for $C_{24}H_{27}N_6O_4$ $[M+H]^+$: 463.2094. Found: 463.2098.

5.3. General procedure for the synthesis of *10a–d*

Amide **9** (25 mg, 0.054 mmol) was added to a vial containing CsF in dry DMSO (3 mL). The mixture was placed in a Biotage® Initiator synthesizer at 100 W for the time indicated in each case. Water (5 mL) was added and the organic phase was extracted with ethyl acetate (3 × 5 mL), dried over $MgSO_4$, filtered and evaporated. The residue was purified by silica gel flash chromatography.

*5.3.1. N-{2-[4-(2-methoxyphenyl)piperazin-1-yl]ethyl}-N-(4-nitropyridin-2-yl)benzamide (**10a**)*

Using CsF (41 mg, 0.27 mmol) and heating for 2.5 min. Ethyl acetate/hexane (4:1) was used as the eluent. Yield: 10 mg, 40%. ^{1}H NMR (500 MHz, $CDCl_3$): δ 8.33 (1H, dd, $J = 5.7$ Hz, $J = 8.7$ Hz, $H6_{py}$), 7.72 (2H, m, $H5_{py} + H_{Ar}$), 7.35–7.30 (3H, m, H_{Ar}), 7.25–7.22 (2H, m, H_{Ar}), 6.96 (1H, td, $J = 2.1$ Hz, $J = 6.0$ Hz), 6.90–6.85 (2H, m, H_{Ar}), 6.82 (1H, dd, $J = 1.1$ Hz, $J = 8.1$ Hz), 7.87 (1H, td, $J = 2.1$ Hz, $J = 5.7$ Hz), 6.58 (1H, dd, $J = 2.1$ Hz, $J = 10.2$ Hz, $H3_{py}$), 4.27 (2H, t, $J = 6.2$ Hz, CH_2NCO), 3.82 (3H, s, OCH_3), 2.96 (4H, br. s, CH_2N), 2.64 (2H, br s, CH_2N), 2.62 (4H, m, 2× CH_2N) ppm. ^{13}C NMR (125 MHz, $CDCl_3$): δ 171.1, 170.8, 168.6 (d, $^1J_{C-F} = 261.7$ Hz, $C4_{py}$), 152.2, 150.3 (d, $^3J_{C-F} = 8.3$ Hz, $C6_{py}$), 141.3, 135.8, 130.5, 128.3, 122.8, 120.9, 118.1, 111.2, 110.0 (d, $^2J_{C-F} = 20.1$ Hz, $C5_{py}$), 109.0 (d, $^2J_{C-F} = 16.6$ Hz, $C3_{py}$), 60.4, 56.5, 55.3, 50.6 ppm. Anal. ($C_{25}H_{28}N_4O_2F$) theoretical: C, 68.95; H, 6.48; N, 12.86. Found: C, 69.26; H, 6.66; N, 12.43. IR (ν_{max}, NaCl): 2941, 2818, 1661, 1574, 1534, 1500, 1465, 1355, 1304, 1240, 1141, 1022, 911, 733 cm^{-1}. HRMS (ESI-TOF): Calculated for $C_{25}H_{28}N_4O_2F$ [M+H]$^+$: 435.2196. Found 435.2196.

*5.3.2. N-(4-fluoropyridin-2-yl)-N-{2-[4-(2-methoxyphenyl)piperazin-1-yl]ethyl}-cyclohexanecarboxamide (**10b**)*

Using CsF (41 mg, 0.27 mmol) and heating for 2.5 min. Ethyl acetate/hexane (4:1) was used as the eluent. Yield: 12 mg, 52%. ^{1}H NMR (200 MHz, $CDCl_3$): δ 8.42 (1H, dd, $J = 3.0$ Hz, $J = 14.5$ Hz, $H6_{pyr}$), 7.19 (1H, dd, $J = 8.7$ Hz, $J = 14.5$ Hz, $H5_{pyr}$), 6.97–6.80 (5H, m, $H_{Ar} + H_{pyr}$), 3.97 (2H, t, $J = 6.6$ Hz, CH_2NCO), 3.82 (3H, s, OCH_3), 2.98 (4H, br s, 2× CH_2N), 2.63–2.56 (6H, m, 3× CH_2N), 2.44 (1H, br. dt, H_{chx}), 1.73–1.07 (10H, m, H_{chx}) ppm. ^{13}C NMR (75 MHz, $CDCl_3$): δ 176.5, 169.4 (d, $^1J_{C-F} = 263.0$ Hz, $C4_{py}$), 158.3 (d, $^3J = 10.5$ Hz, $C6_{py}$), 152.3, 150.8 (d, $^3J = 8.0$ Hz, $C2_{py}$), 141.2, 122.9, 120.9, 118.2, 111.2, 110.1 (d, $^2J = 16.7$ Hz, $C5_{py}$), 109.6 (d, $^2J = 19.2$ Hz, $C3_{py}$), 56.5, 55.4, 53.4, 50.5, 45.1, 42.6, 29.6, 25.6 ppm. Anal. ($C_{25}H_{34}N_4O_2F$) theoretical: C, 68.00; H, 7.76; N, 12.69. Found: C, 68.32; H, 7.97; N, 12.4. IR (ν_{max}, NaCl): 2930, 2816, 1667, 1581, 1501, 1450, 1240, 1135, 1028, 822, 748 cm^{-1}. HRMS (ESI-TOF) Calculated for $C_{25}H_{34}N_4O_2F$ [M+H]$^+$: 441.2666. Found 441.2678.

*5.3.3. N-(4-fluoropyridin-2-yl)-N-{2-[4-(2-methoxyphenyl)piperazin-1-yl]ethyl}-adamantane-1-carboxamide (**10c**)*

Using CsF (82 mg, 0.54 mmol) and heating for 2.0 min. Ethyl acetate was used as the eluent. Yield: 19 mg, 70%. ^{1}H NMR (300 MHz, $CDCl_3$): δ 8.41 (1H, m, $H6_{py}$), 7.07 (1H, dd, $J = 1.9$ Hz $J = 9.5$ Hz, $H5_{py}$), 7.00–6.94 (2H, m, $H5_{py} + H_{Ar}$), 6.90–6.87 (2H, m, H_{Ar}), 6.82 (1H, d, $J = 7.6$ Hz, H_{Ar}), 3.82 (5H, m, $CH_2NCO + OCH_3$), 3.00 (4H, m, 2× CH_2N), 2.60 (6H, m, 3× CH_2N), 1.85–1.48 (15H, m, H_{Ad}) ppm. ^{13}C NMR (75 MHz, $CDCl_3$): δ 179.5, 169.5 (d, $^1J = 263.6$ Hz, $C4_{pr}$), 159.6 (d, $^3J = 9.9$ Hz, $C6_{py}$), 152.2, 150.4, (d, $^3J = 8.1$ Hz, $C2_{py}$), 141.2, 122.8, 120.9, 118.1, 110.7 (d, $^2J = 16.7$ Hz, $C5_{py}$), 110.2 (d, $^2J = 18.0$ Hz, $C2_{py}$), 55.9, 55.3, 53.4, 50.5, 48.8, 44.3, 39.9, 36.4, 28.3 ppm. Anal. ($C_{29}H_{38}N_4O_2F$) theoretical: C, 70.56; H, 7.76; N, 11.35. Found: C, 70.87; H, 7.81; N, 11.08. IR (ν_{max}, NaCl): 2095, 2245, 1644, 1580, 1500, 1451, 1240, 1142, 1026, 911, 731 cm^{-1}. HRMS (ESI-TOF): Calculated for $C_{29}H_{38}N_4O_2F$ [M+H]$^+$: 493.2999. Found 493.3003.

*5.3.4. N-(4-fluoropyridin-2-yl)-N-{2-[4-(2-methoxyphenyl)piperazin-1-yl]ethyl}pyridine-2-carboxamide (**10d**)*

Amide **9d** (40 mg, 0.086 mmol) was added to a vial containing CsF (66 mg, 0.42 mmol) in dry DMSO (2 mL). The vial was placed into a Biotage® Initiator microwave oven and heated for 3 min at 140 °C. Water (5 mL) was added and the organic phase was extracted with ethyl acetate (3 × 5 mL), dried over $MgSO_4$, filtered and evaporated. The residue was purified by silica gel column flash chromatography using ethyl acetate as the eluent. Yield: 23 mg, yellow oil, 62%. ^{1}H NMR (200 MHz, $CDCl_3$): δ 8.29 (1H, d, $J = 4.7$ Hz, $H3_{py}$), 8.21 (1H, dd, $J = 5.5$ Hz, $J = 9.1$ Hz, $H6_{py}$), 7.73 (2H, m, $H5_{py} + H6_{py}$), 7.21 (1H, m, $H4_{py}$), 6.98–6.73 (6H, m, $H_{py} + H_{Ar}$), 4.62 (2H, t, $J = 6.7$ Hz, CH_2NCO), 3.82 (3H, s, OCH_3), 2.93 (4H, m, 2× CH_2N), 2.77 (2H, t, $J = 6.4$ Hz, CH_2N), 2.63 (4H, m, 2× CH_2N) ppm. ^{13}C NMR (75 MHz, $CDCl_3$): δ 168.9 (d, $^1J = 261.1$ Hz, $C4_{py}$), 168.8, 158.6 (d, $^3J = 10.5$ Hz, $C6_{py}$), 153.5, 152.1, 149.9 (d, $^2J = 13.8$ Hz, $C2_{py}$), 148.0, 141.1, 136.8, 124.7, 124.3, 122.8, 120.8, 118.0, 111.0, 109.4 (d, $^2J = 15.0$ Hz, $C5_{py}$), 108.5 (d, $^2J = 19.8$ Hz, $C3_{py}$), 56.3, 55.2, 53.3, 50.5, 45.8 ppm. Anal. ($C_{24}H_{27}N_5O_2F$) theoretical: C, 66.04; H, 6.23; N, 16.04. Found: C, 66.27; H, 6.31; N, 15.90. IR (ν_{max}, NaCl): 2939, 2818, 1660, 1583, 1500, 1385, 1240, 1138, 1025, 856, 747 cm^{-1}. HRMS (ESI-TOF): Calculated for $C_{24}H_{27}N_5O_2F$ [M+H]$^+$: 436.2146. Found 436.2146.

5.4. Radiolabeling

*5.4.1. General procedure for the radiosynthesis of compounds [^{18}F]**10a** and [^{18}F]**10c–d***

No carrier added [^{18}F]F$^-$ (20.6–89.5 GBq) was transferred in a solution of $H_2^{18}O$ (3.6 mL; Rotem Industries) to a TRACERlab MX synthesizer (GE Healthcare) loaded with a modified cassette for FDG synthesis (Rotem Industries). The [^{18}F]F$^-$ ions were trapped on a QMA light cartridge and eluted with a solution of kryptofix K_{222} (22 mg) and K_2CO_3 (7 mg) in H_2O/MeCN (500 μL/500 μL). The solution was dried azeotropically (four cycles at 95 °C) and a solution of the precursor compound (**9a**, **9c–d**; 10–15 mg) dissolved in DMSO (2.5 mL) was added to the reactor. Fluorination was undertaken at 180 °C over 5–10 min and the crude mixture was passed through a pre-activated Sep-Pak C18 column. The column was washed with H_2O and eluted with MeOH (1.5 mL). The eluate was collected and manually injected into an HPLC (semi-preparative, reversed phase column; Spherisorb ODS C18, 250 × 10 mm, 5 μm, 80 Å; H_2O/MeOH/THF = 65:22:13, acidified to pH 5–6; flow rate of 4 mL/min). The purified fraction, identified by comparison with the cold reference, was collected and formulated for injection by dilution with H_2O (20–40 mL), passage through a pre-activated Sep-Pak C18 cartridge and elution of the retained compound with EtOH (2 mL).

*5.4.1.1. [^{18}F]-N-(4-fluoropyridin-2-yl)-N-{2-[4-(2-methoxyphenyl)piperazin-1-yl]ethyl}-benzamide ([^{18}F]**10a**).* Retention time in HPLC: 21 min. The purified compound was isolated and reformulated for injection in 25.7% radiochemical yield (~23 GBq; decay corrected to EOB) and the sample was analyzed by analytical HPLC system (analytical, reversed phase column; ZORBAX Eclipse Plus C18, 150 × 4.6 mm, 5 μm) to determine its radiochemical purity (>99%) and its specific activity (72–450 GBq/μmol).

*5.4.1.2. [^{18}F]-N-(4-Fluoropyridin-2-yl)-N-{2-[4-(2-methoxyphenyl)piperazin-1-yl]ethyl}-adamantane-1-carboxamide ([^{18}F]**10c**).* Retention time in HPLC: 13 min. The purified compound was isolated and reformulated for injection in 25.9% radiochemical yield (~20 GBq; decay corrected to EOB) and the sample was analyzed by analytical HPLC (analytical, reversed phase column; ZORBAX Eclipse Plus C18, 150 × 4.6 mm, 5 μm) to determine its radiochemical purity (>99%) and its specific activity (80–250 GBq/μmol).

*5.4.1.3. [^{18}F]-N-(4-Fluoropyridin-2-yl)-N-{2-[4-(2-methoxyphenyl)piperazin-1-yl]ethyl}-pyridine-2-carboxamide ([^{18}F]**10d**).* Retention time in HPLC: 12 min. The purified compound was isolated and reformulated for injection in 22.7% radiochemical yield

(~18 GBq; decay corrected to EOB) and the sample was analyzed by analytical HPLC (analytical, reversed phase column; ZORBAX Eclipse Plus C18, 150 × 4.6 mm, 5 μm) to determine its radiochemical purity (>99%) and its specific activity (25–60 GBq/μmol).

5.4.2. *[^{18}F]-N-(4-Fluoropyridin-2-yl)-N-{2-[4-(2-methoxyphenyl)piperazin-1-yl]ethyl}-cyclohexanecarboxamide ([^{18}F]**10b**)*

The radiolabeled compound [^{18}F]**10b** was prepared by nucleophilic aromatic substitution of the nitro precursor **9b** with $^{18}F^{-}$ using a Synthera® (IBA Molecular) automated radiosynthesizer loaded with an integrated fluidic processor (IFP; ABX Biochemicals). In a typical procedure, no carrier added [^{18}F]F^{-} (79 GBq) produced by proton bombardment of $H_2^{18}O$ (3.6 mL; Rotem Industries) was transferred to the synthesizer and the anions were retained in a QMA light cartridge. The [^{18}F]F^{-} was eluted to the reactor with a solution of K_2CO_3 (7 mg) and K_{222} (22 mg) in H_2O/MeCN (500 μL/500 μL) and dried at 100 °C and variable pressure over 5 min. A solution of 11 mg of compound **9b** in DMSO (1.2 mL) was reacted with the $K^{+18}F^{-}$ at 180 °C over 8 min. The reaction mixture was cooled and diluted with H_2O (4.5 mL). The solution was subsequently passed through a pre-activated ^{t}C-18 Sep-Pak™ column. After eluting with methanol (1.5 mL), the crude preparation was purified by automated HPLC (semi-preparative, reversed phase column; Luna C18(2), 250 × 10 mm, 5 μm, 100 Å), with a mobile phase consisting of H_2O (65%)/MeOH (22%)/THF (13%), acidified to pH 5.5 (flow rate of 4 mL/min). The typical retention time of [^{18}F]**10b** was 70 min. The compound was formulated for *in vivo* injection by dilution of the HPLC solution with H_2O (40 mL), retention of the compound in a pre-activated ^{t}C-18 Sep-Pak™ column, and elution with ethanol (0.2–1.0 mL). The purified and formulated compound was injected into an analytical HPLC system (analytical, reversed phase column; ZORBAX Eclipse Plus C18, 150 × 4.6 mm, 5 μm) to determine its radiochemical purity (>99%) and its specific activity at the time of product release (110–510 GBq/μmol). The radiochemical yield, corrected to end-of-bombardment (EOB), was 27.8%.

5.5. *[^{18}F]**10b** in vitro brain autoradiography*

Coronal rat brain slices (40 μm thickness placed on glass slides) were incubated with [^{18}F]**10b** (1 μCi/mL in 50 mM Tris–HCl pH 7.5, 20 min). After washing to remove the non-incorporated radioactivity, the slides were dried and apposed on Agfa Curix RP-2 plus films during 1 h. After exposure, the films were manually developed and the images were digitally captured. The binding pattern of [^{18}F]**10b** was identical to those obtained with ligands [^{18}F]MPPF and [^{3}H]8-OH-DPAT, which correspond to the known 5-HT_{1A} receptor rat brain distribution. Furthermore, the specific signal was abolished when the positron emitter tracer was incubated in the presence of a high concentration of cold (non-radioactive) 8-OH-DPAT, WAY-100635 or **10b**.

5.6. *[^{18}F]MPPF displacement*

Male Sprague–Dawley rats ($n = 13$) weighing approximately 200 g were dynamically scanned (25 frames, 45 min) in a PET-CT small animal device (Albira ARS, Oncovision) immediately after injection of [^{18}F]MPPF (approx. 400 μCi (14.8 MBq), i.v.), with increasing doses of cold **10b** (0, 0.01, 0.02, 0.03, 0.075, 0.16 and 0.3 mg/kg). Once the data had been acquired, the tomographic images were reconstructed (by applying the OSEM algorithm) and the binding potential (BP; ratio of Bmax to k_D) was calculated. When calculated *in vitro* (using Pmod 3.0 software), BP is the point at which the concentrations of specifically bound ligand and free ligand are equal.

5.7. *[^{18}F]**10b** dynamic PET*

These studies were carried out to examine the pharmacokinetics and binding behavior of the tracer when evaluated *in vivo*, in order to confirm that the compound crosses the blood–brain barrier and binds to 5-HT_{1A} receptors. The protocol used was almost identical to that described for [^{18}F]MPPF displacement, with the principal difference being that [^{18}F]**10b** was used instead of [^{18}F]MPPF.

5.8. *In vivo displacement of [^{18}F]**10b***

To assess the specificity of [^{18}F]**10b** for 5-HT_{1A} receptors, animal PET studies with [^{18}F]**10b** were performed in the presence of two well-characterized 5-HT_{1A} ligands, namely 8-OH-DPAT and WAY-100635, as well as with cold **10b**. The protocol was again similar to that outlined for [^{18}F]MPPF displacement, with the difference that [^{18}F]**10b** was used as the tracer instead of [^{18}F]MPPF.

5.9. *Biodistribution in rats*

The biodistribution of compound [^{18}F]**10b** was evaluated by injecting it (approx. 500 μCi (18.5 MBq), i.v. via tail vein) into Sprague–Dawley male rats weighing approximately 200 g. The animals were killed by decapitation at 15, 30, 60, and 120 min after injection of the radiotracer. In order to determine the brain uptake another set of rats were killed at just 1 min after injection of the tracer. The organs and tissues were immediately removed and dissected on an ice-cooled glass plate. After dissection, the tissues were submerged and washed in saline solution (0.9% NaCl) to remove adhering blood and the samples were weighed and placed in counting vials. The radioactivity of each sample was measured in a gamma counter (Cobra II Auto-Gamma, Packard; energy window 450–570 KeV, 1 min/vial). The counts per minute (CPM) were corrected by means of a standard calibration curve. Finally, the calibrated activities were expressed as a percentage of injected dose per gram of tissue (%ID/g), taking into account the radioactive decay from the injection until the measurement of the vial.

Acknowledgments

The authors acknowledge the Instituto Tecnológico PET (CENIT-20081013, CDTI UAH-17/2009), Comunidad de Madrid (Projects S-BIO-0170-2006 and S2011/BMD-2349), Ministerio de Economía y Competitividad (Projects CTQ-2008/05027/BQU and SAF2009-09020) and Universidad de Alcalá (Projects UAH2011/EXP-034 and UAH GC2012/001) for financial support. The collaboration of Ms. Mary Brennan in some steps of the synthesis and Rubén Fernández de la Rosa in PET recordings is also acknowledged.

Appendix A. Supplementary data

Supplementary data related to this article can be found at http://dx.doi.org/10.1016/j.ejmech.2014.07.096.

References

[1] J. Borg, Molecular imaging of the 5-HT_{1A} receptor in relation of human cognition, Behav. Brain Res. 195 (2008) 103–111.
[2] F. Yasuno, T. Suhara, T. Ichimiya, A. Takano, T. Ando, Y. Okubo, Decreased 5-HT_{1A} receptor binding in amygdala of schizophrenia, Biol. Psychiatry 55 (2004) 439–444.
[3] W.C. Drevets, E. Frank, C.J. Price, D.J. Kupfer, D. Holt, P.J. Greer, Y. Huang, C. Gautier, C. Mathis, PET imaging of serotonin 1A receptor binding in depression, Biol. Psychiatry 46 (1999) 1375–1387.
[4] V. Arango, Y.-Y. Huang, M.D. Underwood, J.J. Mann, Genetics of the serotonergic system in suicidal behaviour, J. Psychiatr. Res. 37 (2003) 375–386.

[5] G.M. Sullivan, M.A. Oquendo, M. Simpson, R.L. Van Heertun, J.J. Mann, R.V. Parsey, Brain serotonin$_{1A}$ receptor binding in major depression is related to psychic and somatic anxiety, Biol. Psychiatry 58 (2005) 947–954.
[6] J. Tiihonen, A. Keski-Rahkonen, M. Loeppoenen, M. Muhonen, J. Kajander, T. Allonen, K. Nagren, J. Hietala, A. Rissanen, Brain serotonin$_{1A}$ receptor binding in bulimia nervosa, Biol. Psychiatry 55 (2004) 871–873.
[7] M.K.P. Lai, Reduced serotonin 5-HT$_{1A}$ receptor binding in the temporal cortex correlates with aggressive behavior in Alzheimer disease, Brain Res. 974 (2003) 82–87.
[8] V. Kepe, J.R. Barrio, S. Cheng Huang, L. Ercoli, P. Siddarth, K. Shoghi Jadid, G.M. Cole, N. Satyamurthy, J.L. Cummings, G.W. Small, M.E. Phelps, Serotonin$_{1A}$ receptors in the living brain of Alzheimer's disease patients, Proc. Natl. Acad. Sci. U. S. A 103 (2006) 702–707.
[9] S.J. Kish, J. Tong, O. Hornykiewicz, A. Rajput, L.-J. Chang, M. Guttman, Y. Furukawa, Preferential loss of serotonin markers in caudate versus putamen in Parkinson's disease, Brain 131 (2008) 120–131.
[10] J. Passchier, A. Van Waarde, Visualisation of serotonin-1A (5-HT$_{1A}$) receptors in the central nervous system, Eur. J. Nucl. Med. 28 (2001) 113–129.
[11] V.W. Pike, C. Halldin, H.V. Wikström, Radioligands for the study of the brain 5-HT$_{1A}$ receptors in vivo, Prog. Med. Chem. 38 (2001) 189–247.
[12] J.S.D. Kumar, J.J. Mann, PET tracers for 5-TH$_{1A}$ receptors and uses thereof, Drug Discov. Today 12 (2007) 748–756.
[13] V.W. Pike, J.A. McCarron, S.P. Hume, S. Ashworth, J. Opacka-Juffry, S. Osman, A.A. Lammertsma, K.G. Poole, A. Fletcher, et al., Pre-clinical development of a radioligand for studies of central 5-HT$_{1A}$ receptors in vivo-[^{11}C]WAY-100635, Med. Chem. Res. 5 (1995) 208–227.
[14] C.-Y. Shiue, G.G. Shiue, P.D. Mozley, M.-P. Kung, Z.-P. Zhuang, H.-J. Kim, H.F. Kung, p-[^{18}F]-MPPF: a potential radioligand for PET studies of 5-HT$_{1A}$ receptors in humans, Synapse 25 (1997) 147–154.
[15] A. Fletcher, E.A. Forster, D.J. Bill, G. Brown, I.A. Cliffe, J.E. Hartley, D.E. Jones, A. McLenachan, K.J. Stanhope, D.J. Critcheley, K.J. Childs, V.C. Middlefell, L. Lanfumey, R. Corradetti, A.M. Laporte, H. Gozlan, M. Hamon, C.T. Dourish, Electrophysiological, biochemical, neurohormonal and behavioural studies with WAY-100635, a potent, selective and silent 5-HT$_{1A}$ receptor antagonist, Behav. Brain Res. 73 (1996) 337–353.
[16] B.R. Chemel, B.L. Roth, B. Armbruster, V.J. Watts, D.E. Nichols, WAY-100635 is a potent D$_4$ agonist, Psychopharmacology 188 (2006) 244–251.
[17] J.C. Martell, N. Leduc, A.N. Ormiere, V. Faucillon, N. Danty, C. Culie, D. Cussac, A. Newman-Tancredi, WAY100535 has high selectivity for serotonin 5-HT(1A) versus dopamine D(4) receptors, Eur. J. Pharmacol. 574 (2007) 15–19.
[18] Z. Tu, R.H. Mach, C-11 radiochemistry in cancer imaging applications, Curr. Top. Med. Chem. 10 (2010) 1060–1095.
[19] N. Ginovart, W. Hassoun, D. Le Bars, D. Weissmann, V. Leviel, In vivo characterization of p-[^{18}F]MPPF, a fluoro analog of WAY-100635 for visualization of 5-HT$_{1A}$ receptors, Synpase 35 (2000) 192–200.
[20] V.W. Pike, C. Halldin, H. Wikström, S. Marchais, S.P. Hume, M. Constantinou, B. Andree, L. Farde, Radioligands for the study of brain 5-HT$_{1A}$ receptors in vivo-development of some new analogs of WAY, Nucl. Med. Biol. 27 (2000) 449–455.
[21] S. Osman, C. Lunskvist, V.W. Pike, C. Haldin, J.A. McCarron, C.-G. Swahn, L. Farde, N. Ginovart, S.K. Luthra, R.N. Gunn, C.J. Bench, P.A. Sargent, P.M. Grasby, Characterization of the appearance of radioactive metabolites in monkey and human plasma from the 5-HT$_{1A}$ receptor radioligand, [carbonyl-^{11}C]WAY-100635-Explanation of high signal contrast in PET and an aid to biomathematical modelling, Nucl. Med. Biol. 25 (1998) 215–223.
[22] J. Sandell, C. Halldin, V.W. Pike, Y.-H. Chou, K. Varnäs, H. Hall, S. Marchais, B. Nowicki, H.W. Wikström, C.-G. Swahn, L. Farde, New halogenated [^{11}C]WAY analogues, [^{11}C]6FPWAY and [^{11}C]6BPWAY—radiosynthesis and assessment as radioligands for the study of brain 5-HT$_{1A}$ receptors in living monkey, Nucl. Med. Biol. 28 (2001) 177–185.
[23] C. Defraiteur, C. Lemaire, A. Luxen, A. Plenevaux, Radiochemical synthesis and tissue distribution of p-[^{18}F]DMPPF, a new 5-HT$_{1A}$ ligand for PET, in rats, Nucl. Med. Biol. 33 (2006) 667–675.
[24] B. Andree, C. Halldin, V.W. Pike, R.N. Gunn, H. Olsson, L Farde, The PET radioligand [carbonyl-^{11}C]desmethyl-WAY-100635 binds to 5-HT1A receptors and provides a higher radioactive signal than [carbonyl-^{11}C]WAY-100635 in the human brain, J. Nucl. Med. 43 (2002) 292–303.
[25] N. Saigal, R. Pichika, B. Easwaramoorthy, D. Collins, B.T. Christian, B. Shi, T.K. Narayanan, S.G. Potkin, J. Mukherjee, Synthesis and biologic evaluation of a novel serotonin 5-HT$_{1A}$ receptor radioligand, [^{18}F]-labelled mefway, in rodents and imaging by PET in a nonhuman primate, J. Nucl. Med. 47 (2006) 1697–1706.
[26] D.W. Wooten, J.D. Moraino, A.T. Hillmer, J.W. Engle, O.J. DeJesus, D. Murali, T.E. Barnhart, R.J. Nickles, R.J. Davidson, M.L. Schneider, J. Mukherjee, B.T. Christian, In vivo kinetics of [F-18]MEFWAY: a comparison with [C-11] WAY100635 and [F-18]MPPF in the nonhuman primate, Synapse 65 (2011) 592–600.
[27] S. Houle, A.A. Wilson, T. Inaba, N. Fisher, J.N. DaSilva, Imaging 5-HT$_{1A}$ receptors with positron emission tomography: initial human studies with [^{11}C] CPC-222, Nucl. Med. Commun. 18 (1997) 1130–1134.
[28] S. Houle, J.N. DaSilva, A.A. Wilson, Imaging the 5-HT$_{1A}$ receptors with PET: WAY-100635 and analogues, Nucl. Med. Biol. 27 (2000) 463–466.
[29] A.A. Wilson, T. Inaba, N. Fischer, L.M. Dixon, J. Nobrega, J.N. DaSilva, S. Houle, Derivatives of WAY100635 as potential imaging agents for 5-HT$_{1A}$ receptors: syntheses, radiosyntheses, and in vitro and in vivo evaluation, Nucl. Med. Biol. 25 (1998) 769–776.
[30] M. Karramkam, F. Hinnen, M. Berrehouma, C. Hlavacek, F. Vaufrey, C. Halldin, J.A. McCarron, V.W. Pike, F. Dollé, Synthesis of a [6-pyridinyl-^{18}F]-labelled fluoro derivative of WAY-100635 as a candidate radioligand for brain 5-HT$_{1A}$ receptor imaging with PET, Bioorg. Med. Chem. 11 (2003) 2769–2782.
[31] J.A. McCarron, V.W. Pike, C. Halldin, J. Sandell, J. Sovago, B. Gulyas, Z. Cselenyi, H.V. Wikstrom, S. Marchais-Oberwinkler, B. Nowicki, F. Dolle, L. Farde, The pyridinyl-6 position of WAY-100635 as a site for radiofluorination-effect on 5-HT$_{1A}$ receptor radioligand behavior in vivo, Mol. Imaging Biol. 6 (2004) 17–26.
[32] R. Al Hussainy, J. Verbeek, D. van der Born, J. Booij, J. Herscheid, D.M. Koos, Design, synthesis, and in vitro evaluation of bridgehead fluoromethyl analogs of N-{2-[4-(2-methoxyphenyl)piperazin-1-yl]ethyl}-N-(pyridin-2-yl)cyclohexanecarboxamide (WAY-100635) for the 5-HT$_{1A}$ receptor, Eur. J. Med. Chem. 46 (2011) 5728–5735.
[33] R. Al Hussainy, J. Verbeek, D. van der Born, A.H. Braker, J.E. Leysen, R.J. Knol, J. Booij, J. Herscheid, D.M. Koos, Design, synthesis, radiolabelling, and in vitro and in vivo evaluation of bridgehead iodinated analogues of N-{2-[4-(2-methoxyphenyl)piperazin-1-yl]ethyl}-N-(pyridin-2-yl)cyclohexanecarboxamide (WAY-100635) as potential SPECT ligands for the 5-HT$_{1A}$ receptor, J. Med. Chem. 54 (2011) 3480–3491.
[34] D.K. Maiti, P.K. Chakraborty, D.C. Chugani, O. Muzik, T.J. Mangner, H.T. Chugani, Synthesis procedure for routine production of [carbonyl-^{11}C] desmethyl-WAY-100635, Appl. Radiat. Isot. 62 (2005) 721–727.
[35] L. Lang, E. Jagoda, Y. Ma, M.B. Sassaman, W.C. Eckelman, Synthesis and in vivo biodistribution of F-18 labelled 3-cis-, 3-trans-, 4-cis, and 4-trans-fluorocyclohexane derivatives of WAY 100635, Bioorg. Med. Chem. 14 (2006) 3737–3748.
[36] S. Osman, C. Lunskvist, V.W. Pike, C. Haldin, J.A. McCarron, C.-G. Swahn, N. Ginovart, S.K. Luthra, C.J. Bench, P.M. Grasby, H. Wikström, T. Barf, I.A. Cliffe, A. Fletcher, L. Farde, Characterization of the radioactive metabolites of 5-HT$_{1A}$ receptor radioligand, [O-methyl-^{11}C]WAY-100635, in monkey and human plasma by HPLC: comparison of the behaviour of an identified radioactive metabolite with parent radioligand in monkey using PET, Nucl. Med. Biol. 23 (1996) 627–634.
[37] N. Saigal, A.K. Bajwa, S.S. Faheem, R.A. Coleman, S.K. Pandey, C.C. Constantinescu, V. Fong, J. Mukherjee, Evaluation of serotonin 5-HT$_{1A}$ receptors in rodent models using [^{18}F]mefway PET, Synapse 67 (2013) 596–608.
[38] M. Kathri, K.R. Santosh, R. Ranbhor, K. Kishore, M. Tiwari, Synthesis and pharmacological evaluation of [(4-arylpiperazin-1-yl)-alkyl]carbamic acid ethyl ester derivatives as potential anxiolytic agents, Arch. Pharm. Res. 35 (2012) 1143–1152.
[39] E.H. Mörkeved, Synthesis of some derivatives of 4-dialkylamino-2-aminopyridine, J. Prackt. Chem. 322 (1980) 343–347.
[40] S. Ranganathan, Y.B.R.D. Rajesh, I.L. Karle, Novel and efficient synthesis of 2- and 4-N-substituted pyridine N-oxides under solvent-free conditions, Synlett (2007) 1215–1218.
[41] S. Wagaw, S.L. Buchwald, The synthesis of aminopyridines: a method employing palladium-catalyzed C–N bond formation, J. Org. Chem. 61 (1996) 7240–7241.
[42] T. Kubo, C. Katoh, K. Yamada, K. Okano, H. Tokuyama, T. Fukuyama, A mild inter- and intramolecular amination of aryl halides with a combination of CuI and CsOAc, Tetrahedron 64 (2008) 11230–11236.
[43] G.A. Grasa, M.S. Viciu, J. Huang, S.P. Nolan, Amination reactions of aryl halides with nitrogen-containing reagents mediated by palladium/imidazolium salt systems, J. Org. Chem. 66 (2001) 7729–7737.
[44] T. Murai, S. Inaji, T. Takenaka, Syntheses and fluoride-ion-mediated hydrolysis of phosphoroselenoic ester and amides, Heteroat. Chem. 20 (2009) 255–261.
[45] T. Koivula, J. Laine, T. Lipponen, O. Perhola, E.-L. Kämäräänen, K. Bergström, O. Solin, Assessment of labelled products with different radioanalytical methods: study on ^{18}F-fluorination of 4-[^{18}F]fluoro-N-[2-[1-(2-methoxyphenyl)-1-piperazinyl]ethyl-N-2-pyridinyl-benzamide (p-[^{18}F] MPPF), J. Radioanal. Nucl. Chem. 286 (2010) 841–846.
[46] J.G. Mulheron, S.J. Casanas, J.M. Arthur, M.N. Garnovskaya, T.W. Gettys, J.R. Raymond, Human 5-HT$_{1A}$ receptor expressed in insect cells activates endogenous G$_0$-like G protein, J. Biol. Chem. 269 (1994) 12954–12962.
[47] Y.C. Cheng, W.H. Prusoff, Relationship between the inhibition constant (k_i) and the concentration of inhibition which causes 50 percent inhibition (IC$_{50}$) of an enzymatic reaction, Biochem. Pharmacol. 22 (1973) 3099–3108.
[48] J. Kelly, G. García, C. Peña, R. Alajarín, J. Álvarez-Builla, M.A. Pozo, Effect of amide substitution on the radiosynthesis of analogues of WAY 100635, a 5HT$_{1A}$ receptor antagonist, J. Label. Compd. Radiopharm. 56 (2013) S147.
[49] N. Malik, C. Solbach, W. Voelter, H.-J. Machulla, Nucleophilic aromatic substitution by [^{18}F]fluoride at substituted 2-nitropyridines, J. Radioanal. Nucl. Chem. 283 (2010) 757–764.
[50] L. Dolci, F. Dollé, S. Jubeau, F. Vaufrey, C. Crouzel, 2-[^{18}F]fluoropyridines by no-carrier-added nucleophilic aromatic substitution with [^{18}F]FK-K222 – a comparative study, J. Label. Compd. Radiopharm. 42 (1999) 975–985.
[51] M. Karramkam, F. Hinnen, F. Vaufrey, F. Dollé, 2-,3- and 4-[^{18}F]Fluoropyridine by no-carrier-added nucleophilic aromatic substitution with K[^{18}F]F-K222 – a comparative study, J. Label. Compd. Radiopharm. 46 (2003) 979–992.
[52] A. Plenevaux, D. Weissmann, J. Aerts, C. Lemaire, C. Brihaye, C. Degueldre, C. Le Bars, D. Comar, J. Pujol, A. Luxen, Tissue distribution, autoradiography, and metabolism of 4-(2′-methoxyphenyl)-1-[2′-[N-2″-pyridinyl)-p-[(18F)]fluorobenzamido]-ethyl]piperazine (p-[(18)F]MPPF), a new serotonin 5-HT(1A)

antagonist for positron emission tomography: an in vivo study in rats, J. Neurochem. 75 (2000) 803–811.

[53] J. Passchier, A. van Waarde, P. Doze, P.H. Elsinga, W. Vaalburg, Influence of P-glycoprotein on brain uptake of [18F]MPPF in rats, Eur. J. Pharmacol. 407 (2000) 273–280.

[54] S. Lu, J.-S. Liow, S.S. Zoghbi, J. Hong, R.B. Innis, V.W. Pike, Evaluation of [11C] S14506 and [18F]S14506 in rat and monkey as agonist PET radioligands for brain 5-HT1A receptors, Curr. Radiopharm. 3 (2010) 9–18.

[55] P.W. Burnet, S.L. Eastwood, P.J. Harrison, [3H]WAY-100635 for 5-HT1A receptor autoradiography in human brain: a comparison with [3H]8-OH-DPAT and demonstration of increased binding in the frontal cortex in schizophrenia, Neurochem. Int. 30 (1997) 565–574.

[56] X. Khawaja, C. Ennis, M.C. Minchin, Pharmacological characterization of recombinant human 5-hydroxytryptamine1A receptors using a novel antagonist radioligand, [3H]WAY-100635, Life Sci. 60 (1997) 653–665.